Supporting Online Material for

Magnetic compass of birds is based on a molecule with optimal directional sensitivity

Thorsten Ritz, Roswitha Wiltschko, P. J. Hore, Christopher T. Rodgers, Katrin Stapput, Peter Thalau, Christiane R. Timmel and Wolfgang Wiltschko

* to whom correspondence on the theoretical background and the calculations should be addressed.
E-mail: tritz@uci.edu and peter.hore@chem.ox.ac.uk.

** to whom correspondence and requests for material on the experiments with birds should be addressed.
E-mail: wiltschko@bio.uni-frankfurt.de

This PDF file includes:

1. Material and Methods

The orientation tests were performed at the Zoological Institute of the Goethe-Universität in Frankfurt (50°08'N, 8°40'E) during spring migration from 2003 to 2006.

Test birds. European robins breed all over Europe. The northern and eastern populations are nocturnal migrants and winter in the Mediterranean countries. Each year, 12 robins were mist-netted during September in the Botanical Garden and identified as transmigrants of probably Scandinavian origin by their wing length. They were kept individually in housing cages in the bird room over the winter. The photoperiod simulated the natural one until the beginning of December when it was decreased to light:dark (L:D) 8:16. Around New Year, the photoperiod was increased in two steps to L:D 13:11. This induced premature spring migration in early January and allowed us to test the birds from early January to the second half of February.

In 2006, we performed experiments in a static field of 92 μT, 66° inclination, about twice the local geomagnetic field. This field is outside the normal functional window of the avian magnetic compass in Frankfurt (*S1*), but robins quickly adjust to that intensity and orient in such a field after 1 h pre-exposure (*S2*). In order not to stress birds too much by excessive handling before testing, we moved the individuals to be tested in the strong field that evening into a second set of housing cages within a pair of Helmholtz coils increasing the local field to 92 μT about 3 h before the tests began. This allowed them to calm down before they were then brought into the 92 μT test field with and without oscillating fields added (see below). In the 92 μT static field, they were indeed well oriented (see Fig. 3 of the paper, upper right diagram). After the respective tests, they were moved back to their normal housing cages in the bird room.

Test procedure. All birds were tested indoors with the magnetic field providing the only directional cue. Testing took place under 565 nm green light, i.e. in conditions under which robins show excellent orientation using their inclination compass (e.g. *S1, S3-S4*), and followed standard procedures: the birds were tested individually once per day in funnel-shaped PVC cages lined with coated paper where they left scratches as they moved (for details, see e.g. *S5 , S6*). Testing began when the lights went off in the birds' housing room and lasted about 75 min.

Test fields. The test rooms were five wooden buildings where the local geomagnetic field was largely undisturbed. The static magnetic intensity at the testing locations had slightly different values ranging from 46.0 to 47.4 μT. This static field served as a control condition. In 2006, experiments were performed in a static field of 92 μT produced by Helmholtz coils (2 m diameter, 1 m clearance) tilted so that the generated field augmented the local geomagnetic field without affecting its inclination. The inhomogeneity of this field was less than 5% in the area of the test cages.

For most tests, the geomagnetic field was supplemented by oscillating magnetic fields. As in previous experiments, they were produced by a coil antenna mounted horizontally on a wooden frame surrounding a set of four test cages so that the oscillating field had a vertical axis, forming an angle of 24° with the vector of the local geomagnetic field. A high-frequency generator produced an oscillating signal that was amplified and, for frequencies above 1 MHz, fed through a resistance of 50 or 51 Ω to the coil; for frequencies below 1 MHz, we used a different amplifier and an 8 Ω resistance. The coil consisted of a single coaxial cable, with 2 cm of the screening removed opposite the feed. The oscillating field strength was measured daily before each test session using a spectrum analyzer (Hewlett Packard 89410A). For

details on the procedure and the equipment used, see (*S5, S6*). We used the same 1.315 MHz field in all test locations based on the median value of the local field at the test sites. There are no indications for a difference between sites.

If an oscillating field of a given frequency and intensity allows normal orientation, an weaker field of the same frequency will not disrupt orientation either. Hence, due to time constraints, we did not perform tests at 0.658 MHz, 48, 15 and 5 nT, at 1.315 MHz, 150 nT and 2.63 MHz, 5 nT in the geomagnetic field. The same applies to the 92 μT static field at 1.315 MHz, 15 and 5 nT and at 2.63 MHz, 150 nT.

Data analysis and statistics. For data analysis, the coated paper was removed from each cage, divided into 24 sectors, and the scratches per sector were counted double blind. From the distribution of these scratches, we calculated the heading for that particular test. Each bird was tested three times in each set of conditions, and the respective three headings were added to produce a mean vector with the heading α_b and the length r_b for each bird. From the mean headings of 12 birds in each test condition, we calculated second order mean vectors with the heading α_N and the length r_N. These were tested for significant directional preference using the Rayleigh test (*S7*). The data obtained with oscillating fields added are compared with the control data of the respective year by the Mardia Watson Wheeler test (*S7*) for differences in distribution and by the Mann Whitney test applied to the angular differences of the 12 data points from their own mean for differences in variance.

2. Numerical results of the orientation experiments with European robins

All tests performed in a specific year involve the same 12 robins, tested three times in each test condition. Tests in the local geomagnetic field, and, in 2006, in a static 92 μT field without an oscillating field added served as control conditions (C).

In the tables, Median r_b gives the median of the vector lengths of the 12 individual birds based on 3 recordings each, indicating the intra-individual variance; α_N and r_N give the direction and length of the grand mean vector based on the 12 mean headings, indicating the inter-individual variance. The asterisks in the r_N column indicate a significant directional preference by the Rayleigh test (S7); if it is not significant, α_N is given in parentheses. ΔC is the angular difference from the respective control data (C), given in parentheses if the vector in the oscillating field was not significant. The last column indicates whether the difference from the controls is significant. Significance levels: *, $p < 0.05$; **, $p < 0.01$: ***, $p < 0.001$; n.s., not significantly different.

Table S1: Orientation behaviour with oscillating fields of various frequencies, intensity 480 nT, added to the local geomagnetic field (see Fig. 1 in the paper)

Frequency added	Year	*N*	Median r_b	α_N	r_N	ΔC	Signif.?
Static field alone*	2003	12	0.93	16°	0.96***	C	
Static field alone	2004	12	0.93	9°	0.94***	C	
Static field alone	2005	12	0.81	10°	0.87***	C	
Static field alone	2006	12	0.93	10°	0.89***	C	
0.01 MHz	2004	12	0.94	7°	0.94***	-2°	n.s.
0.03 MHz	2005	12	0.95	13°	0.81***	+3°	n.s.
0.10 MHz	2004	12	0.61	32°-212°	0.53*	+23°	*
0.50 MHz	2005	12	0.60	6°-186°	0.55*	-4°	**
0.658 MHz	2006	12	0.41	(48°)	0.13 n.s.	(+38°)	**
1.315 MHz*	2003	12	0.52	(14°)	0.15 n.s.	(-2°)	**
2.63 MHz	2004	12	0.71	(137°)	0.30 n.s.	(+129°)	***
7.0 MHz*	2003	12	0.43	(11°)	0.10 n.s.	(-5°)	**

* Data from (S5, S6) included for comparison

Table 2: Orientation behaviour with oscillating fields of various frequencies and intensities added to the local geomagnetic field and to a field with twice its intensity (see Fig. 2 in the paper)

Frequency	intensity	Year	*N*	Median r_b	α_N	r_N	Δ*C*	Signif.?
Static field of	*46 µT*							
Static field	alone	2004	12	0.93	9°	0.94***	C	
Static field	alone	2005	12	0.81	10°	0.87***	C	
Static field	alone	2006	12	0.93	10°	0.89***	C	
0.658 MHz	150 nT	2006	12	0.93	360°	0.91***	-10°	n.s.
1.315 MHz	48 nT	2004	12	0.61	53°	0.17 n.s.	(+44°)	***
	15 nT	2004	12	0.43	157°	0.13 n.s.	(+147°)	***
	5 nT	2004	12	0.86	11°	0.74***	+2°	n.s.
2.63 MHz	150 nT	2005	12	0.63	34°	0.81***	+24°	n.s.
	48 nT	2005	12	0.89	9°	0.91***	- 1°	n.s.
	15 nT	2005	12	0.96	14°	0.93***	+4°	n.s.
Static field of	*92 µT*							
Static field	alone	2006	12	0.91	15°	0.95***	C	
1.315 MHz	150 nT	2006	12	0.92	13°	0.93***	-2°	n.s.
	48 nT	2006	12	0.88	17°	0.93***	+2°	n.s.
2.63 MHz	48 nT	2006	12	0.35	(102°)	0.25 n.s.	(+87°)	***
	15 nT	2006	12	0.69	(350°)	0.42 n.s.	(-25°)	***
	5 nT	2006	12	0.95	10°	0.98***	- 5°	n.s.

3. Calculation of the reaction product yields of model radical pairs subject to a weak static magnetic field and a much weaker oscillating magnetic field

A crucial result of the behavioral experiments described here is that a strong "Zeeman" resonance is observed at the Larmor frequency, ν_L, that satisfies the resonance condition for conventional electron spin resonance spectroscopy

$$\nu_L \,/\, \mathrm{MHz} = 0.0280\ (B_0 \,/\, \mu\mathrm{T}) \qquad (1)$$

where B_0 is the strength of the external static magnetic field. Our observation that the birds respond particularly sensitively to an applied field oscillating at ~1.3 MHz in a 46 μT static field (the Earth's magnetic field at Frankfurt am Main), and at twice that frequency when placed in a 92 μT field, strongly indicates that we observe a Zeeman resonance. We stated in the main text that this observation indicates the presence of a radical pair, in which one radical is devoid of hyperfine couplings. This statement is based on conceptual arguments and numerical calculations described here.

3.1. Zeeman resonances: principles and model radical pairs

We consider a radical pair with negligible electron-electron exchange and dipolar couplings. Under these conditions, the two radicals undergo independent spin evolution under the influence of their hyperfine and Zeeman interactions, even though the radical pair is formed in, and recombines from, a spin-correlated state.

If one radical (denoted A) has no hyperfine interactions, its electron spin has no internal magnetic interactions and interacts only with the external static and (if present) oscillating magnetic fields, whose intensities we denote B_0 and B_1 respectively. Under the conditions of the experiments reported here, the static magnetic field (B_0 = 46 or 92 μT) is much stronger than the oscillating field ($B_1 \leq 480$ nT). Thus, the interaction with the static field is much stronger than all other magnetic interactions experienced by this radical. The spin energy levels of such a radical are particularly simple: there are just two levels with spacing equal to $h\nu_L$. As such, radical A should behave in exactly the same manner as would a radical devoid of hyperfine interactions in an electron spin resonance experiment performed at high field. Specifically, a radical subject to a strong static field and a much weaker linearly polarized resonant oscillating field (i.e. one that satisfies Eqn (1)) has an electron spin resonance signal that is proportional to $\sin^2\theta$ where θ is the angle between the directions of the two magnetic fields. This property, which holds for essentially all high field electron spin resonance and nuclear magnetic resonance experiments, is quantum mechanical in origin and stems from the angle-dependence of the transition dipole moment for the magnetic resonance transition. When the two fields are perpendicular, the transition is fully allowed and the resonance has maximum intensity. When the fields are parallel, the transition is forbidden and the resonance vanishes. Considering multiple copies of similar radical pairs, as one would expect in a sensory cell, this resonance should be intense (provided θ is not close to zero) because every A-type radical exhibits the same resonant behavior at the same frequency.

In radical B, which does have hyperfine interactions, the spin energy levels will exhibit a variety of spacings that depend in a complex manner on the exact details of the hyperfine interactions and the Zeeman interaction. If radical B has n spin-½ nuclei, it will have 2^{n+1} energy levels. In general, one would not expect there to be an energy level spacing corresponding to the Larmor frequency (i.e. $h\nu_L$), especially when the anisotropy of the hyperfine interactions is taken into consideration. The resonances that do occur for radical B will in general be distributed over a range of frequencies from close to zero up

to a frequency of the order of the root-mean-square hyperfine interaction. Each resonance will correspond to a relatively narrow range of orientations of the radical pair for which there is an appropriate pair of energy levels with the correct energy separation (i.e. $h\nu_L$). Thus, in a set of similar radical pairs, only a fraction of the total radical pair population will be responsible for each resonance, which will therefore be correspondingly weak. As the number of hyperfine interactions in B increases, the number of resonances should increase, but their individual intensities will be weaker still because each pair of energy levels will have a smaller share of the population.

In summary, therefore, for an immobilized radical pair with no hyperfine interactions in one of the radicals, subject to a static field B_0 and an oscillating field B_1 such that $B_1 << B_0$, with negligible electron-electron exchange and dipolar couplings, the spectrum of responses to the oscillating field should be dominated by a prominent resonance at the Larmor frequency (Eqn (1)), which becomes weaker as the directions of the two fields deviate from the perpendicular condition and vanishes when the fields are parallel to one another. All other resonances will be much weaker. This is precisely what is shown in Fig. 4 in the main text (discussed further below) and observed in the behavioural experiments.

To demonstrate that these conclusions are borne out by exact numerical calculations, we now present a few illustrative simulations for model radical pairs. The calculations were performed using the modified γ-COMPUTE algorithm, following exactly the procedure described by (S8). The simulations give Φ_S , which is the fraction of radical pairs that recombine from their singlet state (the "singlet yield"), see (S9). The singlet and triplet states of the radical pair are assumed to recombine with equal first order rate constants. Although not essential, this simplification greatly reduces the computational time required and does not obscure the essential physics. The rate constant k is taken as 2×10^5 s^{-1}, which gives a lifetime ($1/k$) of 5 μs.

Fig. S1 shows $\Delta\Phi_S = \Phi_S(B_0 \,\&\, B_1) - \Phi_S(B_0 \text{ alone})$, which is the difference in the singlet yield with and without the oscillating magnetic field, as a function of the frequency of the oscillating field, between 0.5 and 3.0 MHz. The left-hand panels show $\Delta\Phi_S$ for a radical pair with no magnetic nuclei on radical A and two spin-½ nuclei (e.g. hydrogens) on radical B. Here one observes a resonance at the Larmor frequency (1.4 MHz) when the two fields have different directions, but not when they are parallel. As the second hyperfine interaction is increased (from 5 μT to 1 mT), the frequency of this resonance is unchanged. By contrast, when both radicals have hyperfine interactions, as shown in the right-hand panels for a radical pair with one spin-½ nucleus on each radical, the Zeeman resonance is dramatically affected. As the second hyperfine interaction becomes stronger, the Zeeman resonance first splits into two components and then shifts frequency as well. A hyperfine coupling of only 5 μT is sufficient to ensure that there is no longer a strong resonance at the Larmor frequency.

It is clear that other resonances are present in all panels of Fig. S1, e.g. close to 2 MHz when the angle between the fields increases. These features arise principally from the hyperfine interaction of the first nucleus (500 μT) and are always weaker than the Zeeman resonance at 1.4 MHz. The fact that these hyperfine resonances are relatively strong here is just a feature of the simplicity of the radical pair (which contains only two magnetic nuclei with isotropic hyperfine interactions). As Fig. 4 in the main text illustrates (see also below), when more nuclei are included in the calculation, and the anisotropic components of the hyperfine interactions are added, the resonances at frequencies other than the Larmor frequency become relatively much weaker, as anticipated above. Essentially similar spectra, supporting the same general conclusions, have been obtained for a variety of other model radical pairs (not shown).

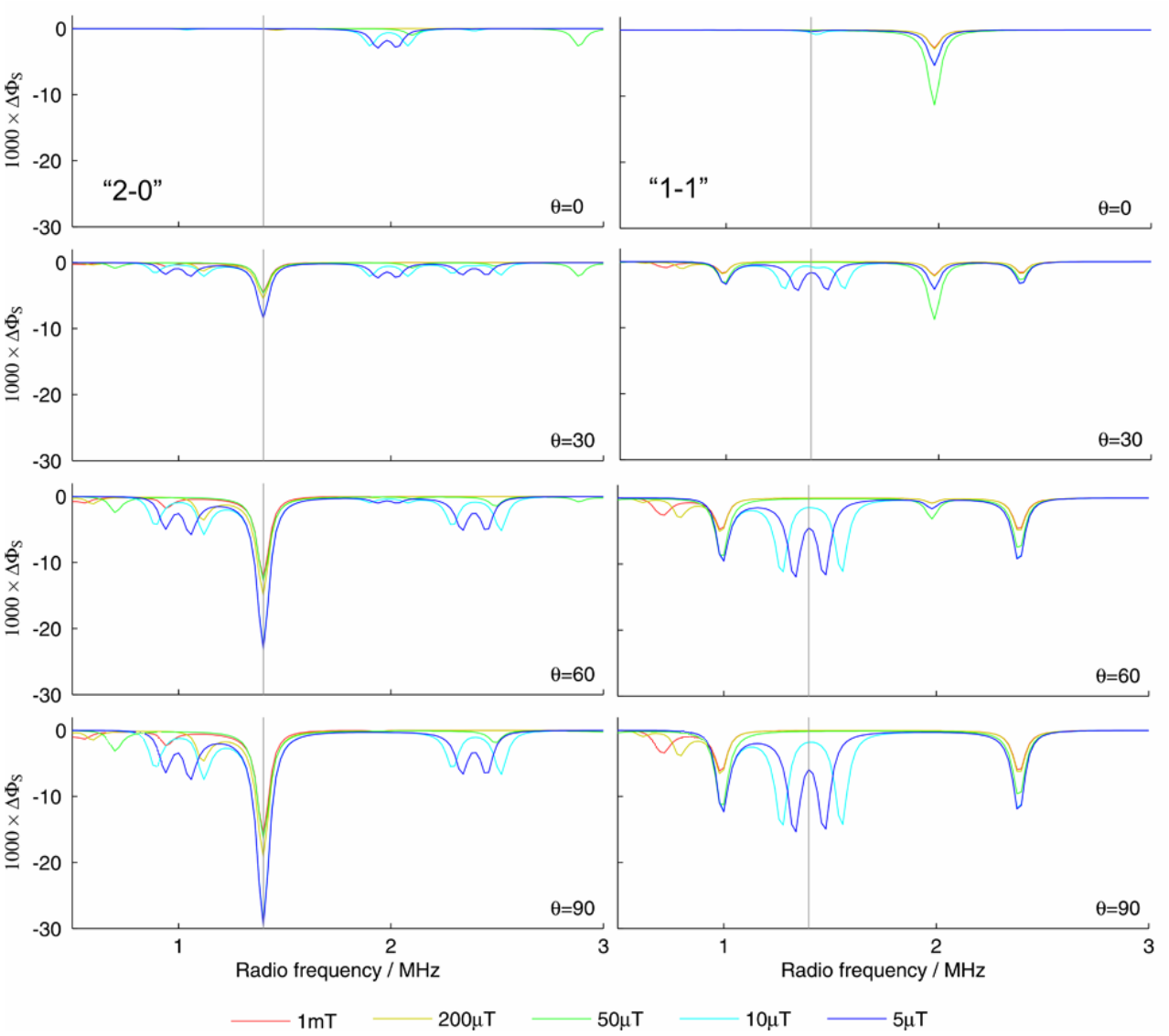

Figure S1. Simulations of $\Phi_S(B_0 \,\&\, B_1) - \Phi_S(B_0 \text{ alone})$, the change in the singlet yield produced by an oscillating magnetic field as a function of the frequency of that field. Left hand panels: radical pairs with two nuclei on one radical and none on the other ("2-0"); right hand panels: radical pairs with one nucleus on each radical ("1-1"). In all panels, one hyperfine interaction is kept fixed at 500 μT while the other is varied as indicated in the legends below. The oscillating field was linearly polarized, and B_0 = 50 μT, B_1 = 700 nT. All hyperfine interactions are isotropic. The angle between the static and radiofrequency magnetic fields changes as indicated in the lower right corner of each panel. The vertical grey lines mark the frequency of the Zeeman resonance, i.e. the Larmor frequency. See text for further details**.**

3.2. Zeeman resonances: anisotropic effects and different static fields

Figure 4 of the main text presents illustrative simulations performed to demonstrate that the spectrum of responses of a more realistic radical pair to an oscillating magnetic field is indeed dominated by the resonance at the Larmor frequency. These calculations differ from those above in that the anisotropic components of the hyperfine interactions are included. As a consequence the anisotropy of the singlet yield must be considered. Note that anisotropic magnetic interactions are vital if a sensor is to detect the direction of an external magnetic field. Without them, the effect of the field on the radical pair reaction

would be isotropic and although this might allow the intensity of the field to be sensed, it would not provide a compass mechanism.

The simulations presented in Fig. 4 of the main text were performed for a model radical pair in which one radical has no hyperfine interactions and the other radical is based on the neutral radical form of flavin adenine dinucleotide, $FADH^{\bullet}$, the radical present in the signalling state of cryptochrome (see paper). This second radical contains the three most significant hyperfine interactions in $FADH^{\bullet}$, namely those for the nitrogens N5 and N10 and the proton H5 (S10). Representations of the anisotropic parts of the hyperfine interactions of N5, N10 and H5 in $FADH^{\bullet}$ are superimposed on the flavin structure in Fig. S2.

The direction of the linearly polarized radiofrequency field (B_1 = 1 μT) made an angle of $\theta = 24°$ with respect to static magnetic field (B_0 = 46 μT or 92 μT). The singlet and triplet states of the radical pair were allowed to recombine with rate constant $k = 5 \times 10^4$ s^{-1}, which gives a lifetime for the radical pair ($1/k$) of 20 μs. The exact values of these parameters are not crucial for the present purpose, which is to demonstrate for the model radical pair described above that (i) there is a Zeeman resonance at the frequency predicted by Eqn (1) and (ii) this resonance is much more intense than the resonances at other frequencies that arise from the $FADH^{\bullet}$ radical. The intention behind these simulations is to illustrate the general behavior of a model radical pair rather than to mimic faithfully the test conditions of the experiments, a task that would be computationally intractable.

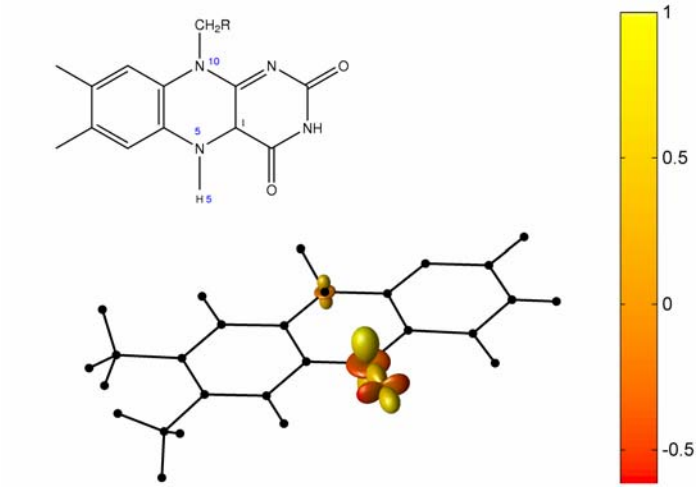

Figure S2. Structure of the flavin radical $FADH^{\bullet}$ and polar plots of the contribution to the energy of the system from the anisotropic hyperfine interactions of nuclei N5, N10 and H5. For each polar plot, the colour scale is indicated on the right hand side from yellow (maximum contribution) to red (minimum contribution). In this way the Figure represents the size and symmetry of the anisotropic parts of the three hyperfine interactions.

Once again, the calculations were performed using the modified γ-COMPUTE algorithm (S8), except that the hyperfine interaction tensors have anisotropic as well as isotropic components. The inclusion of anisotropic magnetic interactions carries with it the requirement to calculate Φ_S for all possible orientations of the radical pair with respect to the directions of the external magnetic field(s), corresponding to all possible orientations of the bird's head with respect to its surroundings. The way in which this is done is by exploiting the Euler angles (α, β, γ) which describe every possible rotation of a three-dimensional shape. For each set of magnetic parameters (B_0, B_1, k, θ, frequency of the oscillating

field, hyperfine interactions) we calculate Φ_S for a total of 4000 values of the three rotation angles in the following ranges: $0 \le \alpha \le 2\pi, 0 \le \beta \le \pi, 0 \le \gamma \le 2\pi$.

A convenient way to handle the complex dependence of Φ_S on the three-dimensional orientation of the radical pair is to separate Φ_S into two components: Φ_S^{iso}, the isotropic (orientation-independent, spherically symmetric) part of the singlet yield, and Φ_S^{an}, the anisotropic (orientation-dependent) part, such that $\Phi_S = \Phi_S^{iso} + \Phi_S^{an}$. From Φ_S^{iso} and Φ_S^{an}, one can calculate two quantities that characterise the change in the singlet product yield caused by the oscillating radiofrequency magnetic field. It is these quantities, which we call Δ_{iso} and Δ_{an}, that are plotted as a function of the frequency of the oscillating field in Fig. 4 of the main text. They are defined as follows.

Δ_{iso} is the change in Φ_S^{iso} produced by the oscillating field divided by Φ_S^{iso} in the absence of the oscillating field:

$$\Delta_{iso} = \frac{\Phi_S^{iso}(B_1 \,\&\, B_0) - \Phi_S^{iso}(B_0 \text{ alone})}{\Phi_S^{iso}(B_0 \text{ alone})}$$

Δ_{an} is the change in the maximum absolute value of Φ_S^{an} produced by the oscillating field divided by the maximum absolute value of Φ_S^{an} in the absence of the oscillating field:

$$\Delta_{an} = \frac{\max\left|\Phi_S^{an}(B_1 \,\&\, B_0)\right| - \max\left|\Phi_S^{an}(B_0 \text{ alone})\right|}{\max\left|\Phi_S^{an}(B_0 \text{ alone})\right|}$$

Typically Δ_{iso} is much larger than Δ_{an}. Δ_{iso} represents the average effect of the oscillating field on the radical pair reaction, while Δ_{an} characterises how the anisotropy of the magnetic field effect is altered by the oscillating field. If the bird becomes disoriented in the presence of the oscillating field it must be as a result of changes in Φ_S that interfere with its perception of the ambient static field. These changes would be reflected in either Δ_{iso} or Δ_{an} or both.

Fig. 4 of the paper displays strong Zeeman resonances at the Larmor frequency in both 46 and 92 μT static fields for both Δ_{iso} and Δ_{an} and very much weaker resonances at other frequencies. Although only the range 1-4 MHz is shown in Fig. 4, the simulations were performed up to 10 MHz revealing only extremely weak additional resonances between 4 and 10 MHz.

References

S1. W. Wiltschko, R. Wiltschko, *J. Comp. Physiol. A* **191**, 675-693 (2005).

S2. W. Wiltschko, K. Stapput, P. Thalau, R. Wiltschko, *Naturwissenschaften* **93**, 300-304 (2006).

S3. W. Wiltschko, R. Wiltschko, *J. Exp. Biol*. **204**, 3295-3302 (2001).

S4. R. Wiltschko, K. Stapput, H. J. Bischof, W. Wiltschko, *Frontiers in Zoology* **4**, 5 (2007).

S5. T. Ritz, P. Thalau, J. B. Phillips, R. Wiltschko, W. Wiltschko, *Nature* **429**, 177-180 (2004).

S6. P. Thalau, T. Ritz, K. Stapput, R. Wiltschko, W. Wiltschko, *Naturwissenschaften* **92**, 86-90 (2005).

S7. E. Batschelet *Circular Statistics in Biology*. (Academic Press, London, 1981).

S8. C. T. Rodgers. K. B. Henbest, P. Kukura, C. R. Timmel, P. J. Hore, *J. Phys. Chem. A* **109**, :5035-5041 (2005).

S9. C. R. Timmel, U. Till, B. Brocklehurst, K. A. McLauchlan, P. J. Hore, *Molec. Phys.* **95**, 71-89 (1998).

S10. F. Cintolesi, T. Ritz, C. W. M. Kay, C. R. Timmel, P. J. Hore, *Chem. Phys.* **294**, 385-399 (2003).